Search for CP Violation in Hyperon Decays at Fermilab

T. Holmstrom [a], and the HyperCP Collaboration

[a]University of Virginia, Charlottesville, VA 22904

The HyperCP collaboration is performing a precision search for CP violation in hyperon decays. Hyperon decays are sensitive to exotic sources of CP violation that kaon decays, for example, are not. The measured CP observable is $A_{\Xi\Lambda} = (\alpha_\Xi\alpha_\Lambda - \alpha_{\overline{\Xi}}\alpha_{\overline{\Lambda}})/(\alpha_\Xi\alpha_\Lambda + \alpha_{\overline{\Xi}}\alpha_{\overline{\Lambda}})$, where α_Ξ and α_Λ are decay parameters for $\Xi^- \to \Lambda\pi^- \to p\pi^-\pi^-$, and $\alpha_{\overline{\Xi}}$ and $\alpha_{\overline{\Lambda}}$ are decay parameters for $\overline{\Xi}^+ \to \overline{\Lambda}\pi^+ \to \overline{p}\pi^+\pi^+$. We report on an analysis of 118 million Ξ^- decays and 42 million $\overline{\Xi}^+$ decays from the 1999 Fermilab fixed-target run, about 10% of the total HyperCP data set, giving a preliminary result of $A_{\Xi\Lambda} = [0.0\pm5.1(\text{stat})\pm4.4(\text{syst})]\times10^{-4}$.

At present non-zero CP asymmetries have been observed only in the decays of K_L [1] and B_d mesons [2]. These results are consistent with standard model predictions but do not preclude other sources of CP violation. Hyperon decays are sensitive to sources of CP violation that neutral kaon decays are not [3,4], in particular parity conserving violations. The difference between spin-1/2 hyperon and anti-hyperon decay distributions in parity-violating two-body weak decays is an interesting place to look for such new CP violation effects. For these particles the angular decay distribution of the daughter baryon in the rest frame of the parent hyperon is

$$\frac{dN}{d\Omega} = \frac{N_0}{4\pi}(1 + \alpha\vec{P}_p\cdot\hat{p}_d), \tag{1}$$

where $\vec{P}_p$ is the parent hyperon polarization, $\hat{p}_d$ is the daughter baryon momentum direction, and $\alpha = 2\text{Re}(S^*P)/(|S|^2 + |P|^2)$, with S and P the angular momentum wave amplitudes. CP symmetry requires that $\alpha = -\overline{\alpha}$ [5].

In HyperCP Ξ^- and $\overline{\Xi}^+$ hyperons were produced with zero average transverse momentum, for which parity conservation in the strong interaction requires that their polarization be zero. The daughter Λ's and $\overline{\Lambda}$'s from $\Xi^- \to \Lambda\pi^-$ and $\overline{\Xi}^+ \to \overline{\Lambda}\pi^+$ decays are then produced in helicity states with their polarization magnitudes given by the parent Ξ^- and $\overline{\Xi}^+$ α decay parameters [6]. The angular distribution of the p's from $\Lambda \to p\pi$ decays becomes

$$\frac{dN}{d\cos\theta} = \frac{N_0}{2}(1 + \alpha_\Xi\alpha_\Lambda\cos\theta), \tag{2}$$

where the polar angle θ is measured in that Λ rest frame, defined so that the polar axis points in the direction of the Λ in the Ξ^- rest frame. If CP is good $\alpha_\Xi = -\overline{\alpha}_\Xi$ and $\alpha_\Lambda = -\overline{\alpha}_\Lambda$, then the angular distribution of the $\overline{p}$ from the decay chain, $\overline{\Xi}^+ \to \overline{\Lambda}\pi^+ \to \overline{p}\pi^+\pi^+$, should be the same as for p in that decay chain.

$$A_{\Xi\Lambda} \equiv \frac{\alpha_\Xi\alpha_\Lambda - \overline{\alpha}_\Xi\overline{\alpha}_\Lambda}{\alpha_\Xi\alpha_\Lambda + \overline{\alpha}_\Xi\overline{\alpha}_\Lambda} \approx A_\Xi + A_\Lambda, \tag{3}$$

where $A_\Xi \equiv (\alpha_\Xi + \overline{\alpha}_\Xi)/(\alpha_\Xi - \overline{\alpha}_\Xi)$ and $A_\Lambda \equiv (\alpha_\Lambda + \overline{\alpha}_\Lambda)/(\alpha_\Lambda - \overline{\alpha}_\Lambda)$. $A_{\Xi\Lambda}$ is almost equal to the sum of A_Ξ and A_Λ, thus any observed asymmetry would come from either the decays of Ξ or Λ but probably both. If A_Ξ and A_Λ were equal and opposite in sign a null result would be observed.

Recent standard model calculations give $-0.5\times10^{-4} \le A_{\Xi\Lambda} \le 0.5\times10^{-4}$ [7] for the combined asymmetry. This prediction uses a theoretical calculation of the S-and P-wave $\Lambda\pi$ final-state scattering phase-shift differences (which must be nonzero for the CP asymmetry to express itself) instead of more recent experimental measurements [8]. Non-standard model calculations, such as left-right symmetric models [9] and some supersymmetric models [10,11], predict the possibility of much larger asymmetries. The supersymmetric calculation of Ref. [10] allows for a value of A_Λ as large as 1.9×10^{-3}. Bounds from

measurements of ϵ and ϵ'/ϵ limit $A_{\Xi\Lambda}$ to be less than 9.7×10^{-3} [4]. The best current experimental limit is $A_{\Xi\Lambda} = +0.012\pm0.014$ [12]. HyperCP is thus the first experiment to test theoretical predictions of $A_{\Xi\Lambda}$ at the $\times10^{-3}$ level.

Data were taken in the 1997 and 1999 Fixed-Target Runs at Fermilab using a high-rate spectrometer [13] (Fig. 1). The hyperons were produced by an 800 GeV/c proton beam, coming from the Tevatron, colliding with a 2×2 mm^2 copper target at zero degrees. Two targets of different lengths were used to balance rates in the spectrometer. After the target was a long curved collimator embedded in a dipole magnet (Hyperon Magnet). Charged particles following the central orbit of the collimator entered the spectrometer at an upward angle of 19.51 mrad to the proton beam with a momentum of 157 GeV/c. Following the collimator was a 13 m long vacuum decay region. After the decay region charged particles were tracked using nine multiwire proportional wire chambers (MWPCs) each with four planes of wires. Two dipole magnets (Analyzing Magnets), placed after the fourth MWPC, bent the decay constituents so that momenta could be determined. At the rear of the spectrometer were two scintillator hodoscopes and a hadronic calorimeter used in the main physics trigger.

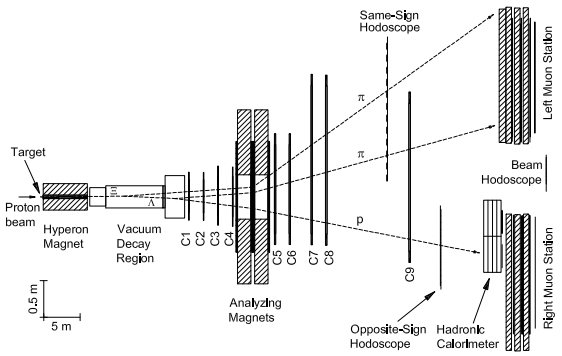

Figure 1. Plan view of the 1999 HyperCP spectrometer.

The 1999 data were taken in a alternating pattern of one Ξ^- (negative) and three $\overline{\Xi}^+$ (positive) runs. Between running modes the polarities of the Hyperon and Analyzing Magnets were reversed and the targets were interchanged. A simple trigger (the CAS trigger) with large acceptance was used to select events with the $\Lambda \to p\pi$ topology. The CAS trigger required the coincidence of at least one hit in each of the hodoscopes (the LR trigger), along with at least $\approx$60 GeV energy deposited in the hadronic calorimeter well below that of the lowest energy p or $\overline{p}$.

The acceptance of the detector causes changes in the $\cos\theta$ distributions, but similar changes for both the p and $\overline{p}$ $\cos\theta$ distributions. Production dynamics result in different Ξ^- and $\overline{\Xi}^+$ momentum and position distributions at the collimator exit, and bias the p and $\overline{p}$ $\cos\theta$ distributions with respect to each other. Two approaches were used to correct for these effects a hybrid Monte Carlo analysis and a weighting analysis. The two techniques provide an important cross-check.

The hybrid Monte Carlo analysis uses a detailed simulation that takes real events as a base and simulates only the Λ decay. Two events were randomly selected from each beam spill during both the 1997 and 1999 runs to provide data to test this approach. An analysis was done using 10 simulated unpolarized Λ decays for each input decay. The Λ decay is simulated using a flat $\cos\theta$ distribution. This distribution is distorted by the acceptance of spectrometer, the inefficiency of the detectors, multiple scattering and the earth's magnetic field; all included in the HMC simulation. The $\cos\theta$ distribution of the HMC events are than adjusted with weights that depend upon the $\alpha_\Xi\alpha_\Lambda$ treated as a parameter to fit the $\cos\theta$ distribution of the real events. The results from 15 million negative events and 30 million positive events give $\alpha_\Xi\alpha_\Lambda = -0.2880\pm0.0004$, with an asymmetry of $A_{\Xi\Lambda}(\text{raw}) = (-7\pm12\pm6.2)\times10^{-4}$.

The weighting analysis, which is the remaining topic of this paper, directly corrects for the acceptance issues by making a ratio of the the p and $\overline{p}$ $\cos\theta$ distributions and than weighting these events to correct for the production differences. The disadvantage of this technique is that no direct measurement of $\alpha_\Xi\alpha_\Lambda$ is made, only the

difference $\alpha_\Xi\alpha_\Lambda - \overline{\alpha}_\Xi\overline{\alpha}_\Lambda$. The advantage is that simulation is only used to check the method not extract the result.

This weighting analysis used 19% of the 1999 positive data (41.4 million events) and 14% of the 1999 negative data (117.3 million events). The data were divided into 18 Analysis Sets, each containing at least three positive and one negative runs taken closely spaced in time. The $p\pi^-\pi^-$

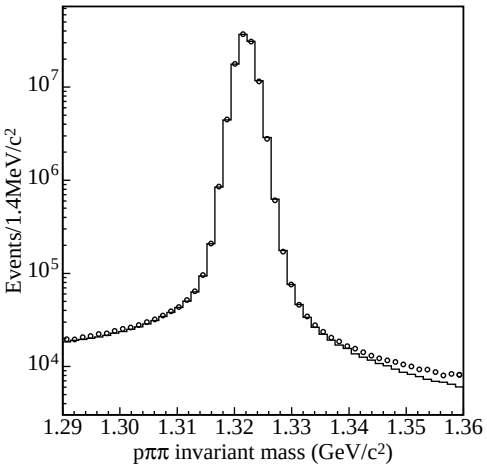

Figure 2. The $p\pi^-\pi^-$ (histogram) and $\overline{p}\pi^+\pi^+$ (circles) invariant masses.

and $\overline{p}\pi^+\pi^+$ invariant masses for these events are shown in Fig. 2, the $\overline{p}\pi^+\pi^+$ data have been scaled up to match the $p\pi^-\pi^-$ data.

The weighting technique binned Ξ^- and $\overline{\Xi}^+$ data in three parameters: the Ξ momentum magnitude (p_Ξ), the Ξ y coordinate (y_Ξ) at the exit of the collimator, and the Ξ y slope ($s_{\Xi y}$) at the exit of the collimator. Each parameter was binned in 100 bins for a total of 10^6 bins. The p_Ξ, y_Ξ, and $s_{\Xi y}$ bin widths were, 2.25 GeV/c, 0.13 mm, and 8.0×10^{-6}. Bins with three or fewer events of either polarity had their weights set to zero. After the weights were computed the p (or $\overline{p}$) $\cos\theta$ of each event was weighted appropriately to form the weighted $\cos\theta$ distributions. The ratio of the weighted p and $\overline{p}$ $\cos\theta$ distributions was taken. The expected form of this ratio

$$R = C\frac{1+\alpha_\Xi\alpha_\Lambda\cos\theta}{1+(\alpha_\Xi\alpha_\Lambda-\delta)\cos\theta}, \qquad (4)$$

determined using Eq. (2), was fit to the data to determine the asymmetry $\delta \equiv \alpha_\Xi\alpha_\Lambda - \overline{\alpha}_\Xi\overline{\alpha}_\Lambda$ and the scale factor C, where the PDG value [14] of $\alpha_\Xi\alpha_\Lambda = 0.294$ was used.

Figure 3 shows a typical ratio of weighted and unweighted proton $\cos\theta$ distributions from one of the Analysis Sets, and Table 1 lists δ for all 18 Analysis Sets. In general fits to R

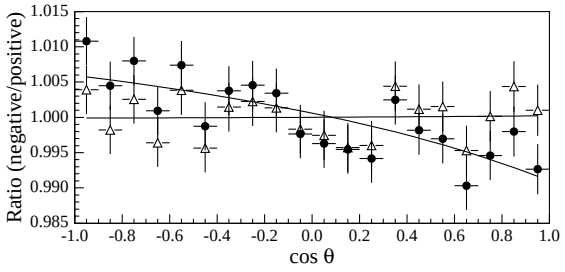

Figure 3. Ratios of p to $\overline{p}$ $\cos\theta$ distributions from Analysis Set 1, both unweighted (filled circles) and weighted (open triangles), with fits to the form given in Eq. (4).

were good; the average χ^2/dof was 0.96. The weighted average of δ for all 18 Analysis Sets is $\delta(\text{raw}) = (-1.3\pm3.0)\times10^{-4}$, where the error is statistical, with $\chi^2 = 24$. The raw asymmetry is $A_{\Xi\Lambda}(\text{raw}) = (2.2\pm5.1)\times10^{-4}$.

The background-corrected asymmetry was determined by measuring the asymmetries of the mass sidebands 1.290 – 1.310 GeV/c^2 and 1.334 – 1.354 GeV/c^2 using the procedure described above, with weights from the central region. The weighted average scaled by the average background fraction of 0.42%, was subtracted from the raw asymmetry to give $A_{\Xi\Lambda} = (0.0\pm5.1)\times10^{-4}$.

The analysis algorithm and its implementation were verified by a simulation, that used momenta

Table 1
Asymmetry δ, statistical error σ, χ^2/dof, and numbers of events for the 18 Analysis Sets.

Analysis Set	δ ($\times 10^{-4}$)	σ ($\times 10^{-4}$)	χ^2/dof	Evts ($\times 10^6$) Ξ^-	$\overline{\Xi}^+$
1	0.8	12.9	0.94	4.6	2.5
2	−20.3	11.1	0.94	10.2	2.8
3	7.2	10.4	0.82	10.4	3.2
4	12.9	11.4	1.56	9.8	2.6
5	−6.6	12.3	0.86	6.8	2.4
6	−25.3	11.1	0.80	5.0	3.8
7	−9.5	10.2	1.37	9.5	3.5
8	19.8	11.0	0.73	9.0	2.9
9	1.1	13.7	1.46	5.2	2.0
10	11.7	12.2	0.75	10.0	2.2
11	−5.3	17.9	0.66	4.0	1.0
12	−27.6	16.6	0.70	4.5	1.2
13	−12.5	13.5	1.04	4.3	2.2
14	−7.5	16.0	0.18	5.8	1.3
15	11.5	15.6	1.15	4.7	1.4
16	−6.9	12.6	1.37	5.2	2.5
17	7.1	13.3	1.56	4.3	2.3
18	27.7	15.0	0.40	4.0	1.6

and positions at the collimator exit from real Ξ^- and $\overline{\Xi}^+$ events as input to computer-generated Ξ decays. This simulation used the earth magnetic field, multiple scatering, and the acceptance of the spectrometer. Using zero and near-zero input asymmetries, the output values of $A_{\Xi\Lambda}$ differed from the input values by $(-1.9\pm1.6)\times10^{-4}$. This value is used as our estimate of the systematic uncertainty due to the validation of the analysis code.

Systematic errors are reduced in this experiment for three reasons. First the direction of the polar angle is different for each event, which means that in general all parts of the decay distribution see all parts of the spectrometer. Second taking a ratio of the p to $\overline{p}\cos\theta$ distributions in the weighting analysis method reduces common biases between the two samples. Finally overall inefficiency differences have no effect on the results only inefficiency differences that have a spatial effect.

The effect of calorimeter inefficiency differences was determined using a data sample taken with the LR trigger. The difference in $A_{\Xi\Lambda}$, with and without the calorimeter trigger requirement, was found to be consistent with zero, with a statistical error of 2.1×10^{-4}. Weighting the real events to correct for the hodoscope inefficiencies changed $A_{\Xi\Lambda}$ by only 0.3×10^{-4}. To estimate the effect of the MWPC inefficiency differences, $A_{\Xi\Lambda}$ was determined from simulations with perfect efficiencies as well as with the real measured efficiencies. The resulting difference in $A_{\Xi\Lambda}$ was 1.0×10^{-4}.

The effect of the uncertainty in the magnetic field of the Analysis Magnet was determined using real data. The analysis was done with a one σ shift in the field for the negative data. The measured difference in $A_{\Xi\Lambda}$ was 2.4×10^{-4}.

The asymmetry $A_{\Xi\Lambda}$ was sensitive to the tight cuts on the Ξ x slope and position at the collimator exit. To study this effect tighter cuts of 4.5% were made on each of these two parameters, which moved $A_{\Xi\Lambda}$ by 1.4×10^{-4} for the x slope cut and 1.2×10^{-4} for the x position cut. The effect of the bin sizes used in extracting the event weights was investigated by both increasing and decreasing the Ξ momentum bin size ($A_{\Xi\Lambda}$ being most sensitive to momentum) by 25% and redoing the base analysis. The larger bin size produced the greatest effect, increasing $A_{\Xi\Lambda}$ by 0.4×10^{-4}. Another possible source of bias was a momentum-dependent differential loss of events due to interactions of the Ξ^- and $\overline{\Xi}^+$ decay products with material in the spectrometer. The effect was modeled using Monte Carlo events and the interaction cross sections given by the PDG [14] and found to be small.

The result was found to be stable with respect to time, Ξ momentum, and secondary-beam intensity. Differences between the Ξ^- and $\overline{\Xi}^+$ production angles could in principle cause a bias due to a difference in production polarizations. Average production angle differences were only $\approx$0.02 mrad. Using the measured production angles, and assuming a linear dependence of the polarization on transverse momentum [15], Monte Carlo studies indicated a negligible effect on the p or $\overline{p}\cos\theta$ slopes. No dependence of $A_{\Xi\Lambda}$ on production angle or incident proton position was evident. The result is also consistent with a sep-

arate HyperCP Hybrid Monte Carlo study done with different data. Table 2 lists the systematic errors. Added in quadrature they give an overall systematic error of 4.4×10^{-4}.

To conclude, we made a preliminary measurement of $A_{\Xi\Lambda}$ to be $[0.0\pm5.1(\text{stat})\pm4.4(\text{syst})]\times10^{-4}$. This result is consistent with standard model predictions and is a factor of twenty improvement over the best previous result [12], and at a level which can began to test theoretical models [10].

Table 2
Systematic errors.

Source	Size ($\times10^{-4}$)
Analyzing Magnets field	2.8
Calorimeter inefficiency	2.1
Validation of analysis code	1.9
Collimator exit x slope cut	1.4
Collimator exit x position cut	1.2
MWPC inefficiency	1.0
Hodoscope inefficiency	0.3
Spectrometer interaction	0.9
Momentum weights bin size	0.4
Background subtraction	0.3
Error on $\alpha_\Xi\alpha_\Lambda$	0.03

The authors would like to thank the staffs of Fermilab and the participating institutions for their vital contributions. This work was supported by the U.S. Department of Energy. E.C.D. and K.S.N. were partially supported by the Institute for Nuclear and Particle Physics. K.B.L. was partially supported by the Miller Institute.

REFERENCES

1. J. Christenson *et al.*, Phys. Rev. Lett. **13**, 138 (1964); A. Alavi-Harati, *et al.*, Phys. Rev. Lett. **83**, 22 (1999); V. Fanti *et al.*, Phys. Lett. B **465**, 335 (1999).
2. For a review, see T.E. Browder and R. Faccini, Annu. Rev. Nucl. Part. Sci. **53**, 353 (2003).
3. N.G. Deshpande, X.-G. He, and S. Pakvasa, Phys. Lett. B **326**, 387 (1994).
4. J. Tandean, Phys. Rev. D **69**, 076008 (2004).
5. A. Pais, Phys. Rev. Lett. **3**, 242 (1959).
6. T.D. Lee and C.N. Yang, Phys. Rev. **108**, 1645 (1957).
7. J. Tandean and G. Valencia, Phys. Rev. D **67**, 056001 (2003).
8. M. Huang *et al.*, Phys. Rev. Lett. **93**, 011802 (2004); A. Chakravorty *et al.*, Phys. Rev. Lett. **91**, 031601 (2003).
9. J.F. Donoghue and S. Pakvasa, Phys. Rev. Lett. **55**, 162 (1985); J.F. Donoghue, X.-G. He, and S. Pakvasa, Phys. Rev. D **34**, 833 (1986); D. Chang, X.-G. He, and S. Pakvasa, Phys. Rev. Lett. **74**, 3927 (1995).
10. X.-G. He, H. Murayama, S. Pakvasa, and G. Valencia, Phys. Rev. D **61**, 071701(R) (2000).
11. C.-H. Chen, Phys. Lett. B **521**, 315 (2001).
12. K.B. Luk *et al.*, Phys. Rev. Lett. **85**, 4860 (2000).
13. R.A. Burnstein *et al.*, hep-ex/0403111, to be published in Nucl. Instrum. and Methods.
14. S. Eidelman *et al.*, Phys. Lett. B **592**, 1 (2004).
15. P.M. Ho *et al.*, Phys. Rev. D **44**, 3402 (1991).